Topological analysis of heterogeneous three-dimensional porous networks: the case of variable connectivity and pore-size correlation

S. Cordero [a], I. Kornhauser [a], C. Felipe [a], J. M. Esparza [a], F. Rojas [a*],
A. Domínguez [a] and J. L. Riccardo [b]

[a]*Departamento de Química, Universidad Autónoma Metropolitana-Iztapalapa
P.O. Box 55-534, México 09340, D.F., México*
[b]*Departamento de Física, Universidad Nacional de San Luis, Chacabuco 917
5700 San Luis, Argentina*

Three-dimensional porous networks, built under the framework of the dual site-bond model of complex substrata, are used to represent the void structure of heterogeneous mesoporous materials. In essence, a topological characterization of different types of simulated porous structures is carried out to visualise therein the effects of: (i) varying connectivity (i.e. the number of throats that emerge from a pore cavity allowing its connection with homologous entities), and (ii) changing pore-size correlation (i.e. how size-alike neighbouring void entities can become). The characterization is based on the evaluation of some statistical properties of the porous substrata such as: (i) the mean size-correlation length between pore elements, and (ii) the connectivity frequency distribution of pore cavities. Through this statistical analysis is found a clear interdependency between local pore connectivity and size-correlation length values. Thus, pore elements display sizes and connectivities that depend on those adopted by their neighbouring void entities. These topological features are explained and discussed in terms of the different morphologies that porous materials can adopt according to the dual site-bond model.

* Corresponding author. Tel. +52 5 8044672, Fax: +52 5 8044666,
E-mail: fernando@xanum.uam.mx

1. INTRODUCTION

A typical porous material is a complex medium made by the arrangement of several billion or trillion void entities per unit mass. The shapes of these entities are, in general, very complicated and pores are intercommunicated via tortuous ways. However, bearing in mind the main morphological properties of these media, one can start simplifying their description by recognizing a characteristic that is common to many of them: the void space can be imaginarily subdivided into a collection of hollow cavities constricted by narrow necks. Subsequently, one could also devise ways to take into account the principal void-to-void interconnection characteristics of the network. Thereafter, the assumption of simple pore shapes instead of the original geometries could provide further simplification, especially with respect to the kind of metric that could be adopted to characterize the sizes of the pore entities. Nowadays most noteworthy modelling of porous media [1 - 9] allow for the existence of the two kinds of pore entities, i.e. cavities and necks, while sometimes involving other important topological properties of porous networks such as variable cavity connectivity [3, 7].

Therefore, a convenient description of a porous medium should be that in which different types of pore structural heterogeneities are considered [7]. Size and connectivity variations are among the most important heterogeneities to be included. Additionally, some other important structural constraints may be introduced according to information proceeding from diverse sources (e.g. electron microscopy).

In this work, a topological analysis (i.e. the way in which void entities are distributed and interconnected throughout the porous medium) of simulated heterogeneous 3-D porous networks will be undertaken. First, a brief description of the Dual Site-Bond Model (i.e. the theoretical foundation on which this study is based) will be made. Afterwards, specific details concerning the Monte Carlo method that will allow us to materialize the theoretical concepts into digital porous networks will be provided. Finally, graphical and tabular results will shed light about the structural order that can exist in different types of porous networks.

2. THEORETICAL BACKGROUND

Heterogeneous mesoporous media of a simplified sort can be constructed through the *Dual Site-Bond Model* (DSBM) of disordered structures [8, 9]. According to this scheme, there are two kinds of void entities that can be recognized in a porous solid: the *sites* (S) and the *bonds* (B). Sites are hollow

cavities or chambers linked to each other by narrower capillaries or bonds. Every site can be interconnected to a variable number C_i of homologous entities. C_i is called the connectivity of the site and also corresponds to the amount of bonds that are surrounding this cavity.

A very important parameter linked to the DSBM and that incorporates the concepts of sites and bonds is the *twofold pore size distribution*: the quantities $F_S(R) \, dR$ and $F_B(R) \, dR$ provide the fractional number of sites and bonds of sizes between R and $R + dR$, respectively. If, for simplicity, sites are assumed as hollow spheres and bonds as open-ended cylinders, then R represents the radius of either a site or a bond. Both distribution functions, $F_S(R)$ and $F_B(R)$, are normalized to unity, so that the fractional number of sites, $S(R)$, or bonds, $B(R)$, of sizes R or smaller are given by:

$$S(R) = \int_0^R F_S(R) \, dR \qquad B(R) = \int_0^R F_B(R) \, dR \qquad (1)$$

The essence of the DSBM resides in the formulation of a *Construction Principle* (CP). In its most basic form, this principle states that the size of any given site in a porous network should be large enough as to accommodate the C_i bonds attached to it. In a more elaborated version, this CP involves that a site size must be larger than, or at most equal to, the size of any of its surrounding bonds, while at the same time these capillaries must not be interfering with each other. For instance, if a pair of orthogonal cylindrical bonds of sizes R_{B1} and R_{B2} meet into a spherical site of size R_S, the site size ought to be:

$$R_S \geq \sqrt{R_{B1}^2 + R_{B2}^2} \qquad (2)$$

Other restrictions can be added to the formulation of the CP depending on further information about the topological properties of the porous structure [10]. Obviously enough, the CP introduces a series of restrictions regarding the parameters of the twofold distribution. One of the most important consequences of the CP is that, in order to construct consistent porous networks, the site-size distribution should be leaned towards larger void sizes than the bond-size distribution. An additional effect related to the latter one is that, depending on the mean connectivity $\overline{C}$ of the porous network, there is a maximum possible overlap (Ω) that can be attained between the site and bond size distributions: the size likeness between cavities and necks can only reach a limiting (maximum) value if all void elements of the twofold distribution are going to be connected together. This Ω is the common area shared by the site and bond distributions and the higher its value the larger the degree of size correlation existing between pore entities.

The relative positions of the site and bond size distributions in a twofold description have led into a classification of porous structures [11]; this classification includes five types of porous media. When $\Omega = 0$ the size of any site is larger than any bond size and types I, II and III are compatible with this characteristic. These three structures are, however, different from each other since type I is one in which F_S and F_B are too far apart, whilst in type III the two functions are very proximate. Type II is intermediate between the former cases. A structure type IV is a situation of non-zero overlap, perhaps the most common occurrence of porous media. Type V is an extreme case of about complete overlap between F_S and F_B, where the adsorbent develops a patch-wise configuration; interconnected sites and bonds of about the same sizes constitute each one of these patches.

3. THE MONTE CARLO METHOD FOR THE CONSTRUCTION OF HETEROGENEOUS POROUS NETWORKS

The Monte Carlo method that allows the materialization of the above concepts into a digital porous network comprises several steps [7].

The first step is to induce the principal characteristics of a porous substrate by choosing an appropriate precursor lattice in which sites and bonds are going to be allocated. For instance, if a cubic lattice is chosen as the precursory network, sites are positioned at the nodes of the arrangement and allowed a maximum connectivity $C_{max} = 6$; besides the node-to-node distance has a fixed length that is at least equal to the diameter of the largest site.

The second step is to establish the parameters of the twofold distribution, i.e. $F_S(R)$ and $F_B(R)$, from which the adequate numbers of sites and bonds will be acquired. The possibility of variable connectivity is introduced via $F_B(R_B)$ by means of a fraction f_0 of virtual or blind bonds (i.e. those entities having $R_B = 0$), this f_0 then adopts the form of a Dirac δ-function. The role of virtual bonds is twofold since, besides of being the tool to impose a given mean connectivity of the porous network, these blind entities help sustaining a more dynamic performance during the following stages of consistency and relaxation of the network, as it will be explained afterwards. Thus, besides $F_S(R)$ we have the following bond size distribution function:

$$F_B(R_B) = \begin{cases} f_0\,\delta(R_B) & \text{for} \quad R_B = 0 \\ F_B'(R_B) & \text{for} \quad R_B > 0 \end{cases} \tag{3}$$

Where $\delta(R_B)$ is a Dirac-δ function arising at $R_B = 0$ and $F_B'(R)$ is the size distribution of real bonds, therefore the following normalization relationship also arises:

$$\int_0^\infty F_B'(R_B)\, dR_B = 1 - f_0 \tag{4}$$

It should be also noted that the mean connectivity $\overline{C}$ depends on f_0 as follows:

$$\overline{C} = C_{max}(1 - f_0) \tag{5}$$

The next step is to set up an initial pore configuration by assigning precise amounts of sites and bonds (i.e. those associated with the chosen twofold distribution) to the precursor lattice. This initialization procedure is carried out at random with no regard of the CP. Because of its arbitrary nature, this initial configuration involves multiple contraventions of the CP; therefore a subsequent combined *consistency* and *relaxation* process is compulsory to perform. This process involves an exhaustive interchange of pore entities in order to generate network configurations that are fully respectful of the CP (i.e. consistent with it) while at the same time void elements are being gradually allocated in the most aleatory possible way (i.e. the network is being relaxed). Details of this combined process are as follows [12]. Firstly, the locations of two sites k and l in the lattice are chosen at random, these entities are swapped if this exchange involves no contradiction of the CP at both places where the cavities are going to be allocated; otherwise the swapping is not performed. This operation is now repeated but on two bonds k and l chosen at random while employing the same criterion: if the exchange between bonds k and l allows the fulfillment of the PC at the two new locations, then the swapping is accepted if not it is rejected. For each swapping attempt exercised on sites, $\overline{C}/2$ attempts should be realized on bonds in order to relax the network steadily. It is also important to say that the entire group of bonds, real and virtual entities, participates in the exchange process. The relaxation procedure is performed according to a number of *Monte Carlo Steps* (MCS); each of these steps involves a number of exchanging attempts (successful or not) that equals the total number of pore elements in the arrangement. For porous networks of about 10^6 elements, the required number of MCS necessary to reach a convenient network, in the sense of fulfilling both the CP and the statistical expectations [13], is of the order of tens of thousands (i.e. tens of thousands of millions swapping operations).

4. RESULTS AND DISCUSSION

The results proceeding from the simulation of heterogeneous porous substrata point to the emergence of two main topological phenomena: (i) a size segregation effect, and (ii) a connectivity segregation effect. The intensities of

these two phenomena depend on the degree of correlation between porous entities, most times influencing very deeply the morphology of a porous substrate. The following analyses will shed light on these topological aspects of heterogeneous 3-D porous networks.

Simulation of porous networks. In order to study the effects of variable size and variable connectivity as well as the degree of correlation between pore entities on the topology of a porous network, a large set of structures was studied in terms of the following parameters: (i) the mean site size $\bar{R}_s$, (ii) the mean bond size $\bar{R}_B$, (iii) the standard deviation σ (assumed to be the same for both sites and bonds, i.e. $\sigma = \sigma_s = \sigma_B$), (iv) the overlap Ω between F_S and F_B, and (v) the mean connectivity $\bar{C}$. σ is a measure of the pore size heterogeneity that exists in the porous structure. In turn, Ω is an indication of the intensity of size correlation between two neighbouring entities. Finally, $\bar{C}$ is a magnitude that not only accounts for the interconnectivity of the porous material but also for the spreading of pore size correlation throughout the network.

Twofold Gaussian distributions in terms of F_S and F_B, and allowing a span of site or bond sizes between $\bar{R} - 3\sigma$ and $\bar{R} + 3\sigma$, have been chosen as the suppliers of the respective pore elements. Besides, F_S and F_B have been set in such a way that the range of pore sizes of the whole void lot is in-between 20-150 Å, an interval credited to mesoporous materials [14]. Table 1 summarizes the sets of Gaussian arrangements that have been constructed, networks with $\bar{C} = 2, 3, 4, 5$ and 6 have been considered. All simulated 3-D porous networks ensued from precursor cubic lattices ($C_{max} = 6$) comprising 80 x 80 x 80 sites together with $3(1-f_0)$ x $(80)^3$ real bonds and $3f_0$ x $(80)^3$ virtual bonds. The following numbers of heterogeneous networks were constructed: 63 for $\bar{C} = 2$, 50 for $\bar{C} = 3$, 43 for $\bar{C} = 4$, 49 for $\bar{C} = 5$ and 33 for $\bar{C} = 6$. Table 1 only shows, for the four bond-size distributions considered in this work, the two extreme mean values between which the myriad of site-size distributions is located, in order to reach a minimum, $\Omega_{min} = 0$, and a maximum, Ω_{max}, overlap with the neck-size distribution, respectively.

Another topological parameter of interest is r_0 the mean size correlation length. This parameter represents the mean length (measured in lattice units and taking the node-to-node distance of the porous lattice as unity) at which the size correlation coefficient $C^{xy}(r)$ (defined below) between two homologous void entities attains a value equal to $1/e$ (i.e. the reciprocal of the natural number e). The correlation length r_0 thus helps measuring the decay of the correlation coefficient with r in multiples of $1/e$. The relationship between r_0 and $C^{xy}(r)$ can be written as [15]:

$$C^{xy}(r) = e^{-r/r_0} \tag{6}$$

Tab. 1. Summary of twofold Gaussian size distribution parameters $\overline{R}_S$, $\overline{R}_B$, σ, $\overline{C}$ and Ω of heterogeneous 3-D porous networks[*]

$\overline{C}$	2	3	4	5	6
$\overline{R}_B = 20$ Å, $\sigma = 4$ Å					
$\overline{R}_{S\ min}$- $\overline{R}_{S\ max}$ (Å)	21–46	25–44	27–44	29–46	32–44
$\Omega_{min} - \Omega_{max}$	0–0.3310	0–0.3580	0–0.3125	0–0.2387	0–0.1366
$\overline{R}_B = 26$ Å, $\sigma = 6$ Å					
$\overline{R}_{S\ min}$- $\overline{R}_{S\ max}$ (Å)	28–62	32- 62	35–62	37–62	42–62
$\Omega_{min} - \Omega_{max}$	0–0.3328	0–0.4052	0–0.3656	0–0.3292	0–0.1839
$\overline{R}_B = 32$ Å, $\sigma = 8$ Å					
$\overline{R}_{S\ m.in}$- $\overline{R}_{S\ max}$ (Å)	34–82	39–82	43–80	50–80	52–80
$\Omega_{min} - \Omega_{max}$	0–0.3330	0–0.4283	0–0.3945	0–0.2384	0–0.2122
$\overline{R}_B = 44$ Å, $\sigma = 12$ Å					
$\overline{R}_{S\ min}$- $\overline{R}_{S\ max}$ (Å)	48–116	56–108	–	68–116	–
$\Omega_{min} - \Omega_{max}$	0–0.3326	0–0.4043	–	0–0.2894	–

[*] $\overline{R}_{S\ max}$ corresponds to the maximum mean size of the site distribution in order to have a zero overlap ($\Omega_{min} = 0$) while $\overline{R}_{S\ min}$ is the minimum mean size of the site distribution to reach a maximum overlap (Ω_{max}) with the given bond-size distribution, respectively

Where $C^{xy}(r)$ is then the correlation coefficient linked to the event of finding sizes R_x and R_y for two homologous void elements x, y, separated by a lattice distance r. $C^{xy}(r)$ and r, are given by:

$$C^{xy}(r) = \frac{\overline{(R_x - \overline{R}_x)(R_y - \overline{R}_y)}}{(\sigma_x^2 \sigma_y^2)^{1/2}} \tag{7}$$

$$r = |\vec{r}_x - \vec{r}_y| \tag{8}$$

Where $\overline{R}_x$, $\overline{R}_y$, σ_x^2 and σ_y^2 are the means and dispersions of R_x and R_y, respectively, while $\vec{r}_x$ and $\vec{r}_y$ are the vectors that define the positions of the two void elements in the lattice. Then, a unitary distance $r = 1$ corresponds to the distance between the centres of two first-order neighbouring sites. When there

is perfect correlation between the sizes of two neighbouring pore entities $C^{xy} = 1$ and $r_0 = \infty$, while $C^{xy} = 0$ implies no correlation and $r_0 = 0$.

Two main size correlation lengths, r_0^{SS} and r_0^{BB}, can be obtained from equations 6 and 7, each of these coefficients quantifying the correlation established between two sites or two bonds separated by a distance r, respectively. In general, $r_0^{SS} \neq r_0^{BB}$ but nevertheless there exists a direct correspondence between them. It is for this reason that r_0^{BB} has been chosen (r_0^{SS} could have also played a similar role) as an adequate parameter to envisage the degree of correlation between void elements in a heterogeneous porous network, and for simplicity it will be just labelled as r_0.

Size correlation between pore elements. Among the three main topological parameters that characterize a heterogeneous porous network, Ω influences the values of r_0 to a larger extent than either $\overline{C}$ or σ [15, 16]. This is because r_0 increases exponentially with Ω, nevertheless the effects of the two other variables ($\overline{C}$ and σ) are not negligible. When σ is small, it is much more probable to find rather extensive pore domains that are constituted by void elements of similar sizes than when this parameter is large. In turn, $\overline{C}$ is a quantity that greatly influences the propagation of correlations between pore entities, thus a large connectivity spreads much more efficiently the size likeness among pore elements throughout the void arrangement.

Figure 1 shows a set of curves of r_0 versus Ω according to different values of $\overline{C}$ and σ. The analysis of the whole set of curves leads to the conclusion that, in general, $\overline{C}$ influences more strongly than σ the outcome of r_0. When $\Omega < 0.1$, the values of $\overline{C}$ and σ have almost no influence on r_0, the overlap and the correlation length are both very small thus meaning that sites and bonds are arranged mostly at random throughout the porous network since the size of any site is in general much larger than the size of any bond. However, when $\Omega > 0.1$ an intense growth of r_0 starts taking place especially for large $\overline{C}$ values. High connectivity promotes strong correlations between pore elements and a *size-segregation effect* [13] becomes apparent. The case of $\overline{C} = 2$ is an interesting one, since here it is possible to attain quite large values of Ω that are very close to the maximum possible limit of this parameter (i.e. $\Omega_{max}(\overline{C} = 2) = 1 - f_0 = 0.333$), under these circumstances the porous network then becomes extremely correlated and the r_0 curve is almost vertical around this value. This is the first evidence of a tubular network being set up at $\overline{C} = 2$, in which case the sizes of interconnected bonds and sites almost coincide, thus forming a substrate of rather long cylindrical capillaries.
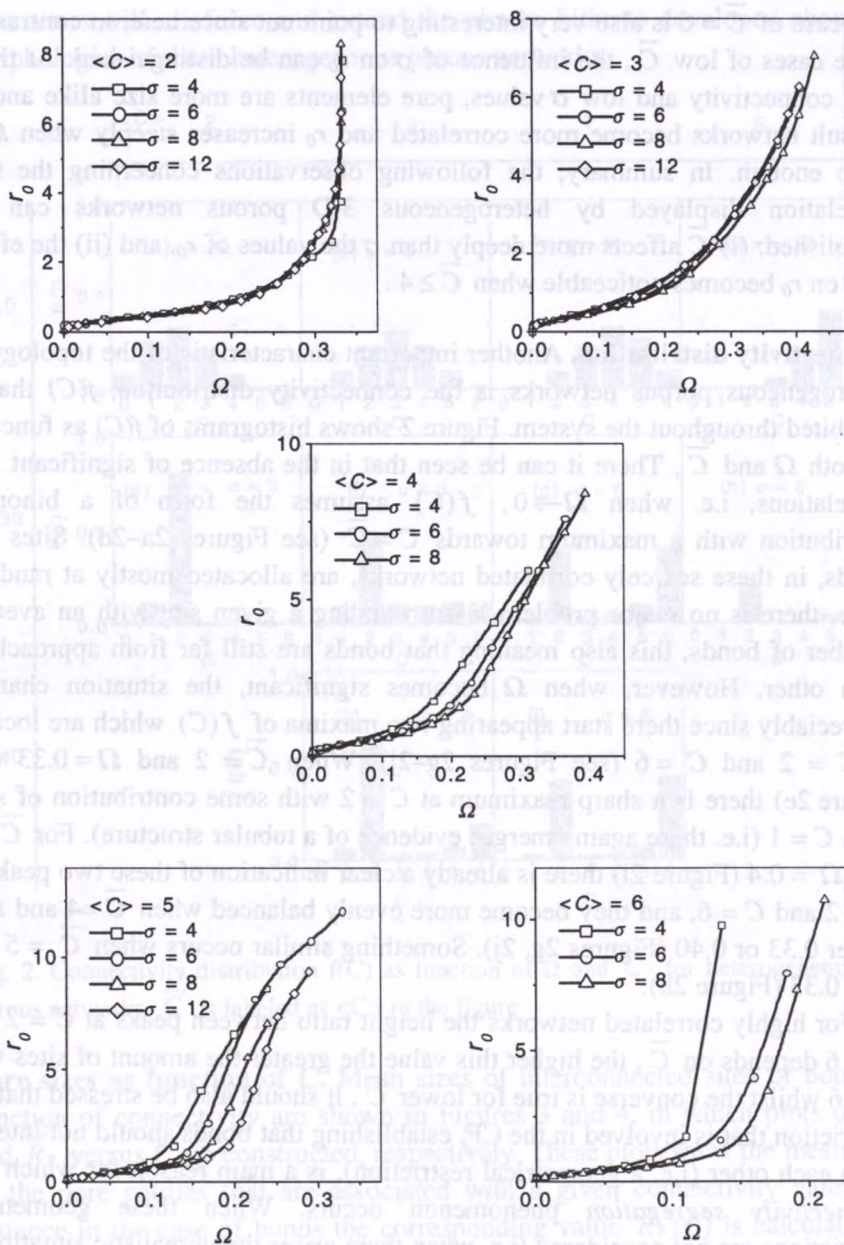
Fig. 1. Correlation length r_0 versus Ω for different $\overline{C}$ values. $\overline{C}$ is labelled as <C> in the plots

The case of $\overline{C} = 6$ is also very interesting to point out since here, in contrast to those cases of low $\overline{C}$, the influence of σ on r_0 can be distinguished. At these high connectivity and low σ values, pore elements are more size alike and as a result networks become more correlated and r_0 increases steeply when Ω is large enough. In summary, the following observations concerning the size correlation displayed by heterogeneous 3-D porous networks can be established: (i) $\overline{C}$ affects more deeply than σ the values of r_0, and (ii) the effect of σ on r_0 becomes noticeable when $\overline{C} \geq 4$.

Connectivity distribution. Another important characteristic of the topology of heterogeneous porous networks is the connectivity distribution, $f(C)$ that is exhibited throughout the system. Figure 2 shows histograms of $f(C)$ as function of both Ω and $\overline{C}$. There it can be seen that in the absence of significant size correlations, i.e. when $\Omega \to 0$, $f(C)$ assumes the form of a binomial distribution with a maximum towards $C = \overline{C}$ (see Figures 2a–2d). Sites and bonds, in these scarcely correlated networks, are allocated mostly at random. Here, there is no major problem in surrounding a given site with an average number of bonds, this also meaning that bonds are still far from approaching each other. However, when Ω becomes significant, the situation changes appreciably since there start appearing two maxima of $f(C)$ which are located at $C = 2$ and $C = 6$ (see Figures 2g–2j). When $\overline{C} = 2$ and $\Omega = 0.33$ (see Figure 2e) there is a sharp maximum at $C = 2$ with some contribution of sites with $C = 1$ (i.e. there again emerges evidence of a tubular structure). For $\overline{C} = 3$ and $\Omega = 0.4$ (Figure 2i) there is already a clear indication of these two peaks at $C = 2$ and $C = 6$, and they become more evenly balanced when $\overline{C} = 4$ and Ω is either 0.33 or 0.40 (Figures 2g, 2j). Something similar occurs when $\overline{C} = 5$ and $\Omega = 0.33$ (Figure 2h).

For highly correlated networks the height ratio between peaks at $C = 2$ and $C = 6$ depends on $\overline{C}$, the higher this value the greater the amount of sites with $C = 6$ whilst the converse is true for lower $\overline{C}$. It should also be stressed that the restriction that is involved in the CP, establishing that bonds should not interact with each other (i.e. a geometrical restriction), is a main reason for which this *connectivity segregation* phenomenon occurs. When these geometrical restrictions are not considered (i.e. when there arises the unrealistic situation in which bonds have the opportunity of interpenetrating each other around the sites) the effect of Ω on $f(C)$ is not so evident [7] and no dominant connectivity values arise. In the following sections, calculation of some other structural

parameters will reinforce and extend the picture hitherto developed about the morphologies of these heterogeneous porous networks.
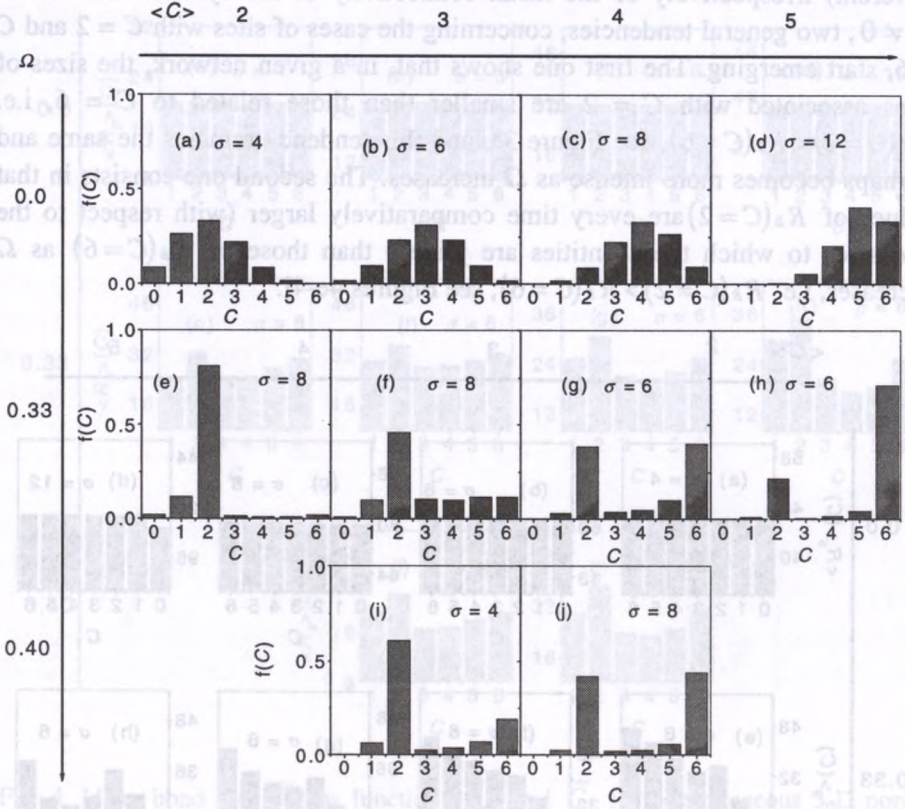

Fig. 2. Connectivity distribution f(C) as function of Ω and $\overline{C}$ for heterogeneous 3-D porous networks. $\overline{C}$ is labeled as <C> in the figure

Pore sizes as function of C. Mean sizes of interconnected sites or bonds as function of connectivity are shown in Figures 3 and 4, in which plots of $\overline{R}_S$ and $\overline{R}_B$ versus C are constructed, respectively. These plots show the mean sizes of the pore entities that are associated with a given connectivity value; for instance in the case of bonds the corresponding value $\overline{R}_B(C)$ is calculated by averaging all bond sizes that are connected to sites of connectivity equal to C, while the site sizes associated with a given C, i.e. $R_S(C)$, is the average size of all these entities depicting the same C. When $\Omega = 0$ there is a uniform distribution of both sites and bonds for every C value, there is no preference at any given region of the porous network for a specified pore size

(see Figures 3a-3d and 4a–4d). Void entities of all possible sizes are interconnected in the same proportions (although their total numbers are different) irrespectively of the mean connectivity of the system. Now when $\Omega \neq 0$, two general tendencies, concerning the cases of sites with $C = 2$ and $C = 6$, start emerging. The first one shows that, in a given network, the sizes of sites associated with $C = 2$ are smaller than those related to $C = 6$, i.e. $R_S(C=2) < R_S(C=6)$, see Figure 3e, and this tendency remains the same and perhaps becomes more intense as Ω increases. The second one consists in that values of $R_B(C=2)$ are every time comparatively larger (with respect to the site sizes to which these entities are joined) than those of $R_B(C=6)$ as Ω increases, i.e. $R_B(C=2) > R_B(C=6)$, see Figures 4e-4j.
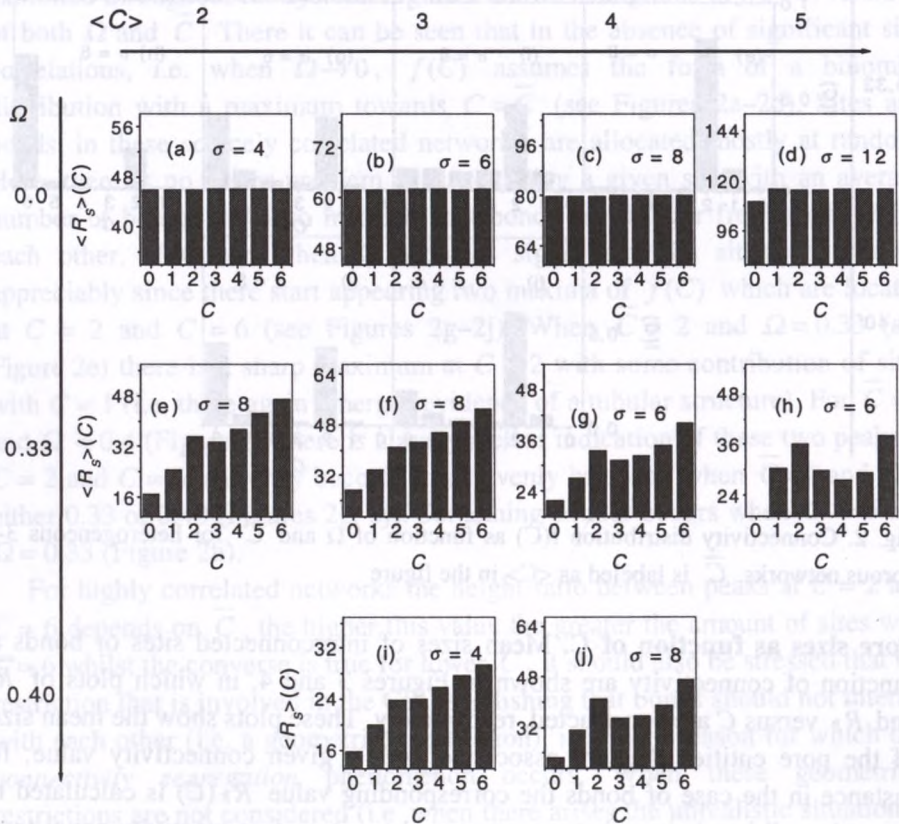
Fig. 3. Mean site size $\overline{R}_s$ as function of Ω and $\overline{C}$ for heterogeneous 3-D porous networks. $\overline{R}_s$ is labelled as <R_S> and $\overline{C}$ is labelled as <C> in the plots
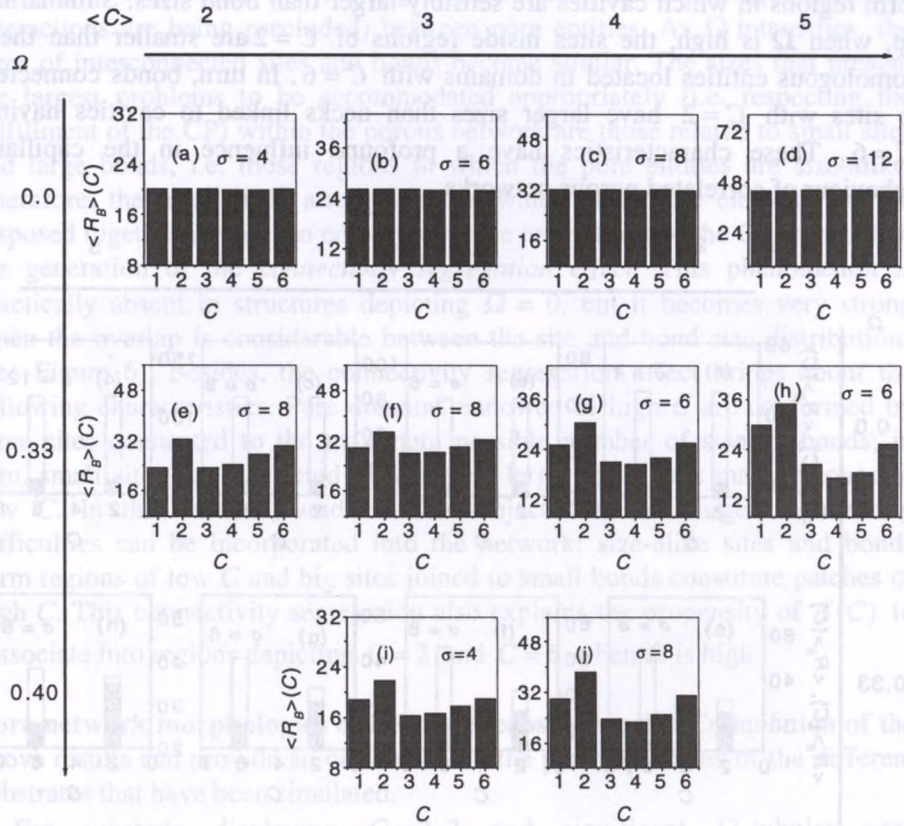
Fig. 4. Mean bond size $\overline{R}_B$ as function of Ω and $\overline{C}$ for heterogeneous 3-D porous networks. $\overline{R}_B$ is labelled as <RB> and $\overline{C}$ is labelled as <C> in the plots

Another important characteristic is the relationship existing between the mean sizes of interconnected sites and bonds for a given $\overline{C}$, i.e. $R_S(C)$ and $R_B(C)$, as function of Ω. Figure 5 depicts a series of plots relative to the mean sizes adopted by both sites and bonds for the cases $C = 2$ and $C = 6$; bar heights at each of these two C values represent the mean sizes of sites (blank bars) and bonds (dashed-filled bars) that are joined together. It can be observed that values of $R_S(C = 2)$ and $R_B(C = 2)$ become more similar as Ω is enlarged, whilst the magnitudes of $R_S(C = 6)$ and $R_B(C = 6)$ remain very different from each other, i.e. $R_S(C = 6) >> R_B(C = 6)$. This means that, when there are appreciable size correlations between pore entities, those pores having similar sizes aggregate together in regions with $C = 2$, whilst those sites with $C = 6$

form regions in which cavities are sensibly larger than bond sizes. Summaring up, when Ω is high, the sites inside regions of $C = 2$ are smaller than their homologous entities located in domains with $C = 6$. In turn, bonds connected to sites with $C = 2$ have larger sizes than necks linked to cavities having $C = 6$. These characteristics have a profound influence in the capillary behaviour of correlated porous networks.
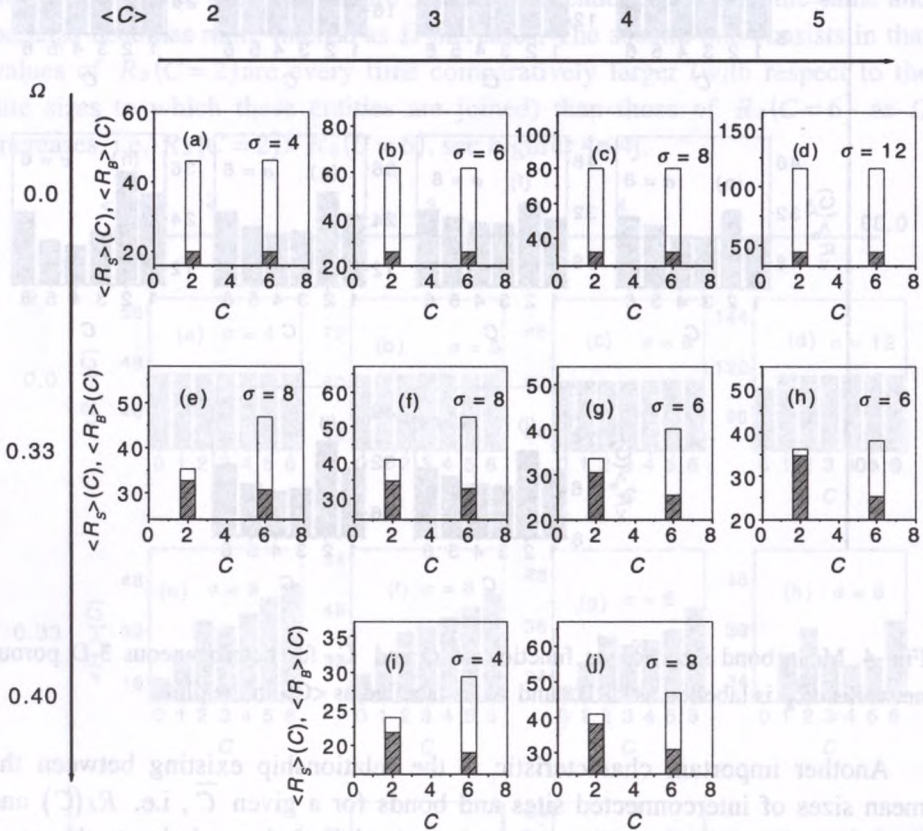

Fig. 5. Mean sizes of sites $\overline{R}_S$ and bonds $\overline{R}_B$ associated with connectivity values of $C = 2$ and $C = 6$. $\overline{R}_S$ (blank bars) is labelled as $<R_S>$, $\overline{R}_B$ (dashed bars) is labelled as $<R_B>$ and $\overline{C}$ is labelled as $<C>$ in the plots.

Bond interactions (geometrical restrictions). The above features of finding comparatively smaller bonds linked to sites when C is high, and also that of having relatively small sites connected to bonds of about the same size when C is low, find their origins in both the existence of strong size correlation and

geometrical restrictions (i.e. these geometrical constraints arising when bond interactions are being precluded) between pore entities. As Ω intensifies, the sizes of interconnected sites and bonds become similar. The sizes that present the largest problems to be accommodated appropriately (i.e. respecting the fulfillment of the CP) within the porous network are those related to small sites and large bonds, i.e. those regions in which the pore entities are size-alike. Therefore, the most likely arrangement in which these pore elements can be disposed together in order to comply with the restrictions of the CP, consists in the generation of the *connectivity segregation effect*. This phenomenon is practically absent in structures depicting $\Omega = 0$, but it becomes very strong when the overlap is considerable between the site and bond size distributions (see Figure 6). Besides, the connectivity segregation effect brings about the following characteristics. Pore domains endowed of high C are conformed by large sites connected to the maximum possible number of smaller bonds; in turn, small sites are connected to relatively large bonds thus making zones of low C. In this fashion, void entities subjected to the largest connecting difficulties can be incorporated into the network: size-alike sites and bonds form regions of low C and big sites joined to small bonds constitute patches of high C. This connectivity segregation also explains the propensity of $f(C)$ to dissociate into regions depicting $C = 2$ and $C = 6$ when Ω is high.

Pore network morphologies of heterogeneous networks. Compilation of the above results can provide an outlook about the pore topologies of the different substrates that have been simulated.

For substrata displaying $C = 2, 3$ and significant Ω, tubular pore morphologies (zones of $C = 2$) are preferentially formed. In these zones, bonds merge with sites of about the same size thus conforming tubular capillaries. Another aspect of this situation consists in that the extent of these regions depends largely on Ω rather than on σ. The tubes are principally arranged as long cylinders with some cross-linking existing between them (see Figure 7a) and when this latter situation occurs this is due to a number of large sites that are fully connected to very small bonds ($C = 6$).

For substrata having $\overline{C} \geq 4$ and moderate values of Ω, there exist pore domains formed by pore entities of similar sizes. The extent of these regions depends very much on σ, the larger the value of this parameter the smaller the extent of each size domain. High C values will be the most abundant within each region; however there also exists some provision of lowly connected pore entities that are mainly located at the borders between the former patches.
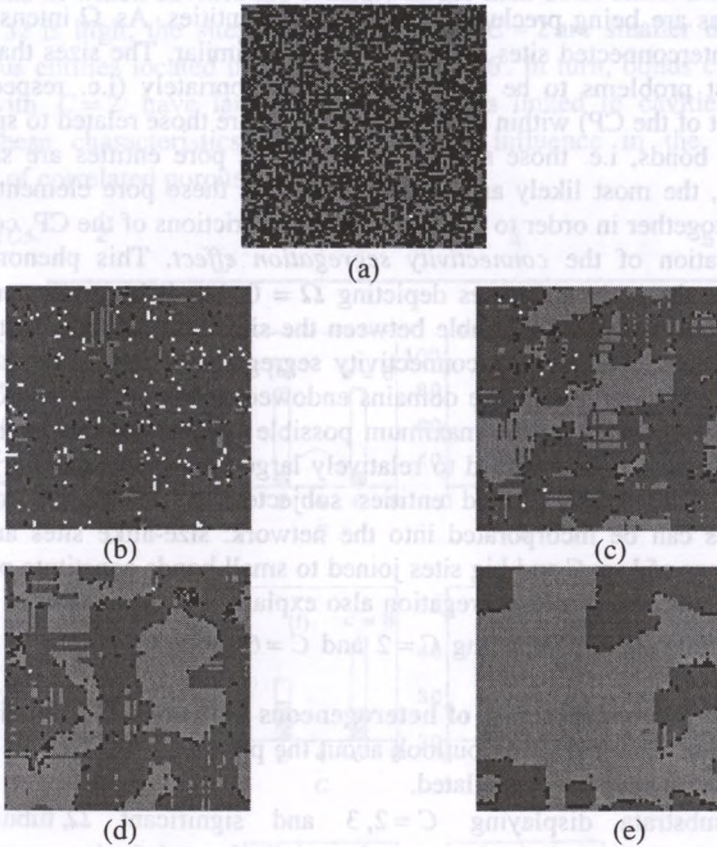
(a)

(b)   (c)

(d)   (e)

Fig. 6. Graphical representation of the site connectivity distribution existing in some 3-D porous networks. Cross-sectional planes comprising 80 x 80 sites containing: (i) poorly connected, C = 5, 6 (dark grey), (ii) medially connected, C = 3, 4 (black) and (iii) highly connected, C = 5, 6 (light grey) pores, are shown. All networks have $\overline{R}_B$ = 26 Å, $\sigma_S = \sigma_B$ = 6 Å. (a) $\overline{C}$ = 4, Ω = 0, $\overline{R}_S$ = 62 Å, (b) $\overline{C}$ = 2, Ω = 0.33, $\overline{R}_S$ = 28 Å, (c) $\overline{C}$ = 3, Ω = 0.40, $\overline{R}_S$ = 32 Å, (d) $\overline{C}$ = 4, Ω = 0.36, $\overline{R}_S$ = 35 Å, (e) $\overline{C}$ = 4, Ω = 0.33, $\overline{R}_S$ = 37 Å

The morphology of a porous network with $\overline{C}$ = 4 and Ω = 0.36 is shown in Figure 7b; this figure corresponding to a close-up of a region formed by 12 x 12 sites and associated bonds. There it can be seen a tubular zone ($\overline{C}$ = 2, left hand side of Figure 7b) separated from a zone of ink-bottles ($\overline{C}$ = 6, right hand side of Figure 7b).
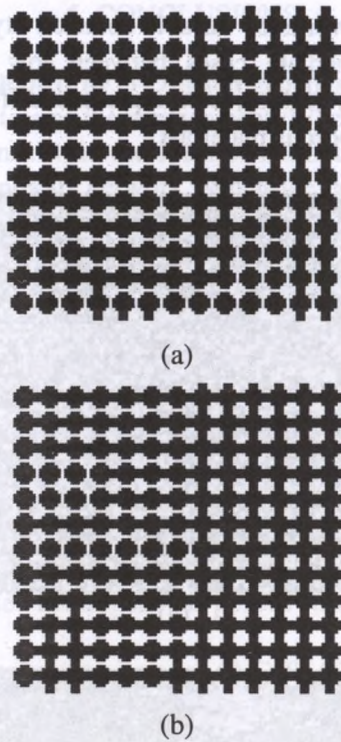
(a)

(b)

Fig. 7. Close-ups of cross-sectional planes of 3-D networks comprising 12 x 12 sites and related bonds, showing topological details of porous media. Sites are represented as black-filled spheres and bonds as black-filled cylinders. (a) Tubular structure related to a network with $\overline{C}$ = 2 and Ω = 0.33, (b) mixed (tubular + ink-bottle) morphology for $\overline{C}$ = 4 and Ω = 0.36

In the case highly of correlated substrata corresponding to $\overline{C} = 2$ or $\overline{C} = 5$, these networks structuralize themselves according to different patterns. Tubular structures are associated with $\overline{C} = 2$ while ink-bottle structures (a large cavity surrounded by narrower bonds) are mostly formed when $\overline{C} = 5$. Networks of constant connectivity, in this case those in which $C = 6$ exist as ink-bottle networks and when Ω is large a *size segregation effect* structuralizes the network into a patch wise substrate of different sizes. Figure 8 exemplifies the appearance of this size segregation effect, since from being not very detectable in networks with $C = 6$ and $\Omega = 0$ (Figure 8a), it becomes very evident in networks with the same C but with a considerable overlap between the site and bond distributions (Figure 8b). This size segregation effect is not exclusive of networks having constant C but it can also arise (together with the connectivity

segregation effect) in networks of variable connectivity and high Ω.. Finally, it can be said that intermediate cases between low (i.e. $\overline{C} = 2$) and high (i.e. $C = 6$) connectivity values, can represent different hybrid (tubular + ink-bottle) topologies of porous materials.
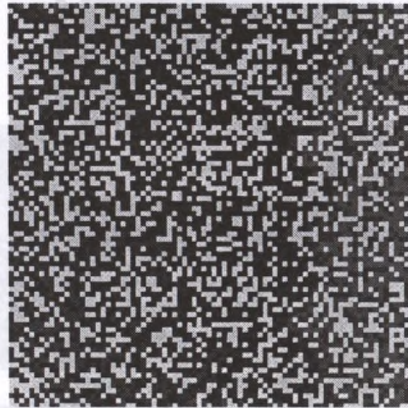
(a)
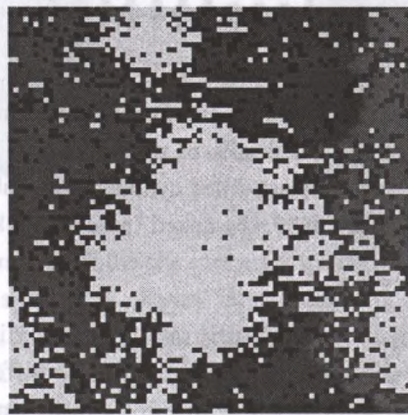
(b)

Fig. 8. Graphical representation of the size-segregation effect that can occur in regular porous networks with C = 6. Cross sectional planes of 3-D porous network comprising 80 x 80 sites are shown. Small sites are represented in grey colour, medium-size ones in black and big voids in white. (a) $\Omega = 0$, $\overline{R}_S = 62$ Å, $\overline{R}_B = 26$ Å, $\sigma_S = \sigma_B = 6$ Å, (b) $\Omega = 0.40$, $\overline{R}_S = 32$ Å, $\overline{R}_B = 26$ Å, $\sigma_S = \sigma_B = 6$ Å

5. CONCLUSIONS

The morphologies adopted by 3-D heterogeneous porous networks depend on the structural parameters of the arrangement. When sites and bonds are very different in size, pore entities in the form of ink-bottle shapes are disposed at random throughout the porous network. When the correlation in size between sites and bonds is high, the structure of porous networks is susceptible to the appearance of two phenomena: a size segregation effect and a connectivity segregation effect. When the latter phenomena occur, the substrate structuralizes itself into a collection of patches having pores of about the same sizes or the same connectivities; these patches alternate with others of different characteristics thus conforming a patch-wise adsorbent. Depending on the mean connectivity of the porous network, the morphologies of these highly correlated substrata can become tubular (low C, high Ω), mixed (tubular + ink-bottle; intermediate C, high Ω) or ink-bottle shaped (high C, high Ω). The overlap between the site and bond distributions as well as the restrictions of geometrical nature play essential roles towards the establishment of network morphologies in correlated heterogeneous porous structures.

REFERENCES

[1] C. D. Tsakiroglou and A. C. Payatakes, *J. Coll. Interf. Sci.* 146, 479 (1991)
[2] V. N. Burganos and A. C. Payatakes, *Chem. Eng. Sci.* 47, 1383 (1992)
[3] G. N. Constantinides and A. C. Payatakes, *Chem. Eng. Comm.* 81, 55 (1989)
[4] C. D. Tsakiroglou A. C. Payatakes, *Adv. Water Res.* 23, 773 (2000)
[5] V. Mani and K. K. Mohanty, *J. Coll. Interf. Sci.* 187, 45 (1997)
[6] M. A. Ioannidis, and I. Chatzis, *J. Coll. Interf. Sci.* 161, 278 (1993)
[7] A. J. Ramírez–Cuesta, S. Cordero, F. Rojas, R. J. Faccio and J. L. Riccardo, *J. Porous Mater.* 8, 61 (2001)
[8] V. Mayagoitia, M. J. Cruz and F. Rojas, *J. Chem. Soc. Faraday Trans. 1* 85, 2071(1989)

[9] V. Mayagoitia, F. Rojas, I. Kornhauser and H. Pérez-Aguilar,
     Langmuir 13, 1327 (1997)
[10] V. Mayagoitia, F. Rojas, I. Kornhauser, G. Zgrablich, R. J. Faccio,
     B. Gilot and C. Guiglion, *Langmuir* 12, 1207 (1996)
[11] V. Mayagoitia, F. Rojas and I. Kornhauser, *J. Chem. Soc. Faraday
     Trans. 1* 84, 785 (1988)
[12] J. L. Riccardo, W. A. Steele, A. J. Ramírez-Cuesta and
     G. Zgrablich, *Langmuir* 13, 1064 (1997)
[13] M. J. Cruz, V. Mayagoitia, and F. Rojas, *J. Chem. Soc. Faraday
     Trans. 1* 85, 2079 (1989)
[14] K. S. W. Sing, D. H. Everett, R. A. W. Haul, L. Moscou, R. Pierotti,
     J. Rouquerol and T. Siemieniewska, *Pure Appl. Chem.* 57, 603 (1985)
[15] J. L. Riccardo, V. Pereyra and G. Zgrablich, *Langmuir* 9, 2730 (1993)
[16] R. H. López, A. M. Vidales and G. Zgrablich, *Langmuir* 16, 3441
     (2000)

CURRICULUM VITAE
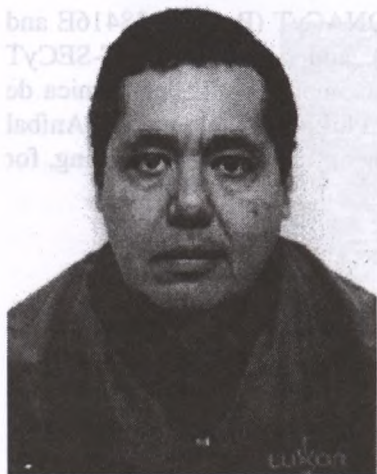
Fernando Rojas-Gonzalez. Date and place of birth: 13 August 1952, Mexico City, Mexico. Married with Silvia Padilla. 2 daughters: Rubi and Silvia Rojas.
Address: Departamento de Quimica, Universidad Autónoma Metropolitana-Iztapalapa,
P. O. Box 55 - 534. C. P. 09340. Mexico, D. F. Telephone: +52 5 8044672, Fax: +52 5 8044666, E-mail: femando@xanum.uam.mx
EDUCATION:
Ph. D. (Surface Chemistry and Colloids). School of Chemistry, University of Bristol (1982). M. Sc. (Surface Chemistry and Colloids). School of Chemistry, University of Bristol (1980). M. Sc (Chemistry). Universidad Autónoma Metropolitana-Iztapalapa (1978). B. Sc. (Chemical Engineering). Escuela Superior de Ingenieria Quimica. Instituto Politecnico Nacional (Mexico).
ACADEMIC APPOINTMENTS:
- Lecturer in Chemistry, Universidad Autónoma Metropolitana-Iztapalapa (1977 - present).
- Head of the Department of Chemistry. Universidad Autónoma Metropolitana-Iztapalapa (1993 - 1996).

- Ph. D. Program Coordinator. Faculty of Basic Science and Engineering. Universidad Autónoma Metropolitana-Iztapalapa (1 991-1993).
- M. Sc. Chemistry Program Coordinator. Faculty of Basic Science and Engineering. Universidad Autónoma Metropolitana-Iztapalapa (1988 - 1991).
- Research Director. Group of Physical Chemistry of Surfaces. Universidad Autónoma Metropolitana-Iztapalapa (1983 - 1988).

SCIENTIFIC DISTINCTIONS:

- Member of the National System of Researchers of Mexico (1 987 - present).
- Visiting Professor, (1) Universidad Nacional de San Luis, Argentina (1987, 1998, 2000), (2) Instituto de Fisica, Universidad Nacional Autónoma de Mexico (2000), (3) Department of Chemistry, University of Reading, U.K. (2001).
- Referee of Journal of Molecular Catalysis (2000).
- Responsible for Scientific Projects awarded by the National Science and Technology Council of Mexico and the Ministry of Education of Mexico to the Group of Physical Chemistry of Surfaces, Department of Chemistry, Universidad Autónoma Metropolitana - Iztapalapa (1996 - present).
- Member of the Scientific Committee of the Fourth International Symposium "Effects of Surface Heterogeneity in Adsorption and Catalysis on Solids" ISSHAC-P/ (2001).